A NOVEL SPECTRAL LINEAR TRANSFORMATION TO ESTIMATE NON-PHOTOSYNTHETIC VEGETATION COVERAGE IN NORTH ASIAN STEPPE

Wenqing Wang [1], Xuehong Chen [1, 2, *], Xin Cao [1], Jin Chen [1, 2]

[1] State Key Laboratory of Earth Surface Processes and Resource Ecology, Faculty of Geographical Science, Beijing Normal University, Beijing 100875, China - chenxuehong@bnu.edu.cn
[2] Beijing Engineering Research Center for Global Land Remote Sensing Products, Institute of Remote Sensing Science and Engineering, Faculty of Geographical Science, Beijing Normal University, Beijing 100875, China

Commission III

KEY WORDS: Non-Photosynthetic Vegetation, Spectral Linear Transformation, Moderate Resolution Imaging Spectroradiometer, North Asian Steppe

ABSTRACT:

Non-Photosynthetic Vegetation (NPV) coverage is an important parameter for wildfire danger rating, prevention of soil erosion and carbon sequestration estimations. A group of spectral indices have been developed to map NPV distribution based on hyperspectral data or particular application scenarios. However, the NPV coverage estimated by those indices are not stable because they are sensitive to soil moisture or snow cover. This paper aims to develop a spectral linear transformation named as Non-photosynthetic Vegetation Index (NPVI) based on Moderate Resolution Imaging Spectroradiometer (MODIS) data to estimate non-photosynthetic vegetation (NPV) coverage in north Asian steppe. The validation result of field spectral experiment and field survey shows the NPVI has good potential to estimate NPV coverage and are robust to soil moisture and snowmelt. Furthermore, the seasonal variation of NPVI offers the possibility to monitor the wildfire risk and grazing intensity.

1. INTRODUCTION

Non-Photosynthetic Vegetation (NPV) consists of dry/dead grasses, plant litter, dead foliage and dead wood. NPV coverage in steppe is an important parameter for many applications including prevention of soil erosion, wildfire danger rating, carbon sequestration estimations and nutrient cycling (Daughtry et al., 2005). A group of spectral indices have been developed to map NPV distribution. For example, hyperspectral cellulose absorption index (CAI) (Elmore et al., 2005; Nagler et al., 2003) can well extracts NPV coverage based on the special peak of lignocellulose absorption around 2100 nm, however its requirement on narrow-width spectral bands limits its application on most available satellite sensors. Other Indices using wide-width spectral bands, such as Dead Fuel Index (DFI), Normalized Difference Index (NDI) and Soil Adjusted Corn Residue Index (SACRI) (Cao et al., 2010; McNairn and Protz, 1993; Biard et al., 1995; Van Deventer et al.,1997), could discriminate NPV in particular scenarios. For example, indices based on Landsat Thematic Mapper (TM) (e.g. NDI, SACRI) were proposed to retrieve NPV coverage in NPV-soil mixture scenario by employing the absorption feature of cellulose in short wavelength infrared (SWIR) bands. Unfortunately, they often fail due to the landscape consisting of more land cover components, like the mixture of Photosynthetic Vegetation (PV), soil and NPV (Xu et al., 2014). Moreover, Landsat sensors cannot reveal the seasonal variation of NPV due to its low revisiting frequency. Remote sensor at coarser spatial resolution, e.g. Moderate Resolution Imaging Spectroradiometer (MODIS), offer the possibility of monitoring seasonality of NPV thanks to its higher revisiting frequency. Dead Fuel Index (DFI) developed for the landscape of three-component mixture (NPV, PV and soil) has been used to estimate the NPV coverage based on MODIS imagery, which is expressed as:

$$\mathrm{DFI} = 100 \cdot (1 - \frac{R_7}{R_6}) \frac{R_1}{R_2} \quad (1)$$

where R_1, R_2, R_6 and R_7 are the reflectance of MODIS bands 1, 2, 6 and 7, respectively. This index combines the spectral reflectance peak in near infrared (NIR) band of PV, and absorption valley of SWIR band of NPV; and is able to estimate NPV coverage in the dry season when the wildfire risk is high. However, DFI developed based on spectral mixture model lacks verifications in the scenarios that includes more complex land cover components and seasonal variations. Especially, DFI of snow cover exhibits very high value, thus overestimates NPV for the scenario with snow cover. Besides, the spectral absorption features of cellulose employed by the above indices are somehow overlapped with the water absorption feature, leading to the sensitivity to soil moisture. Thus, these indices fail to capture the seasonal variation of NPV due to their sensitivity to soil moisture or snow cover (Quemada and Daughtry, 2016). The most NPV indices proposed previously were designed based on the expert experience on several spectral features of limited components, thus often work poorly in more complex scenarios. In this study, instead, we attempt to develop a novel index through learning from a large spectral set with more land cover components and larger spectral variations. The influence of soil moisture variation and snow-cover contamination were considered when establishing the spectral set. Then, the simplest learning method, multiple linear regression model, was used to derive a novel linear spectral transformation for MODIS data to estimate NPV based on the established spectral set.

* Corresponding author

2. METHODOLOGY

The novel linear spectral transformation named as Non-Photosynthetic Vegetation Index (NPVI) is developed based on the combination of spectral mixture simulation and multiple linear regression model in this study. The flowchart is shown in Fig.1.

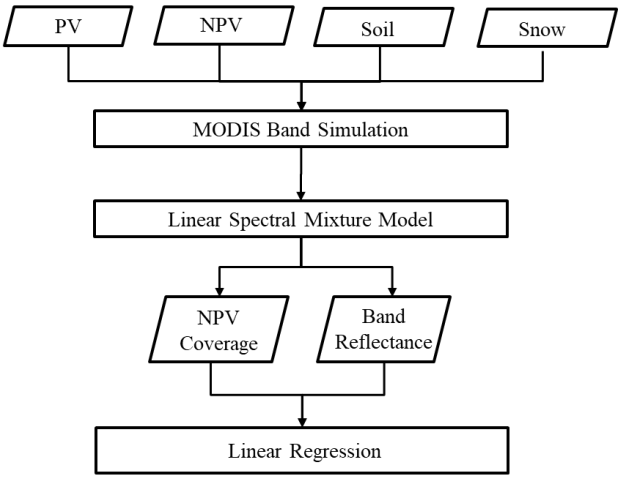

Fig.1 Development of NPVI

First, typical endmember spectra of NPV, PV, soil with different moisture and snow were collected by Analytical Spectral Devices (ASD) Field Spec Pro spectroradiometer (Fig.2). The four kinds of PV spectra represent the main green vegetation species in north Asian steppe. The soil moisture of selected soil spectra was ranged from 2.43% to 25.78% considering the rainfall and snowmelt. Second, the endmember spectra were resampled with MODIS spectral response function. Third, mixed spectra were simulated by combining these endmembers and randomly generated coverages. The linear spectral mixture model could be expressed as:

$$R_{mix} = f_{NPV}R_{NPV} + f_{PV}R_{PV} + f_{soil}R_{soil} + f_{snow}R_{snow} \quad (2)$$

$$\text{subject to: } f_{NPV} + f_{PV} + f_{soil} + f_{snow} = 1$$

where R_{mix} refers the reflectance of mixture at MODIS band 1 to 7. R_{NPV}, R_{PV}, R_{soil} and R_{snow} are the reflectance of each component after resampling with MODIS spectral response function. f_{NPV}, f_{PV}, f_{soil} and f_{snow} are the fraction of each component. They are range from 0 to 1. The distribution of the randomly generated fraction is shown Fig. 3.

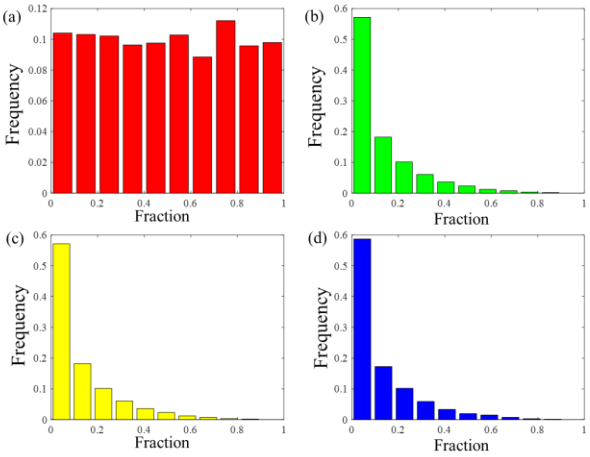

Fig.3 The distribution of generated fractions: (a) NPV; (b) PV; (c) soil; (d) snow.

Finally, a linear transformation of MODIS bands was acquired by regression between simulated NPV coverage and mixed spectra, which is expressed as:

$$\text{NPVI} = 0.2 + 10.7R_1 + 4.1R_2 + 3.6R_3 - 16.0R_4 \quad (3)$$
$$-10.6R_5 + 17.0R_6 - 10.7R_7$$

where R_1 to R_7 are the reflectance of MODIS bands 1 to 7, respectively.

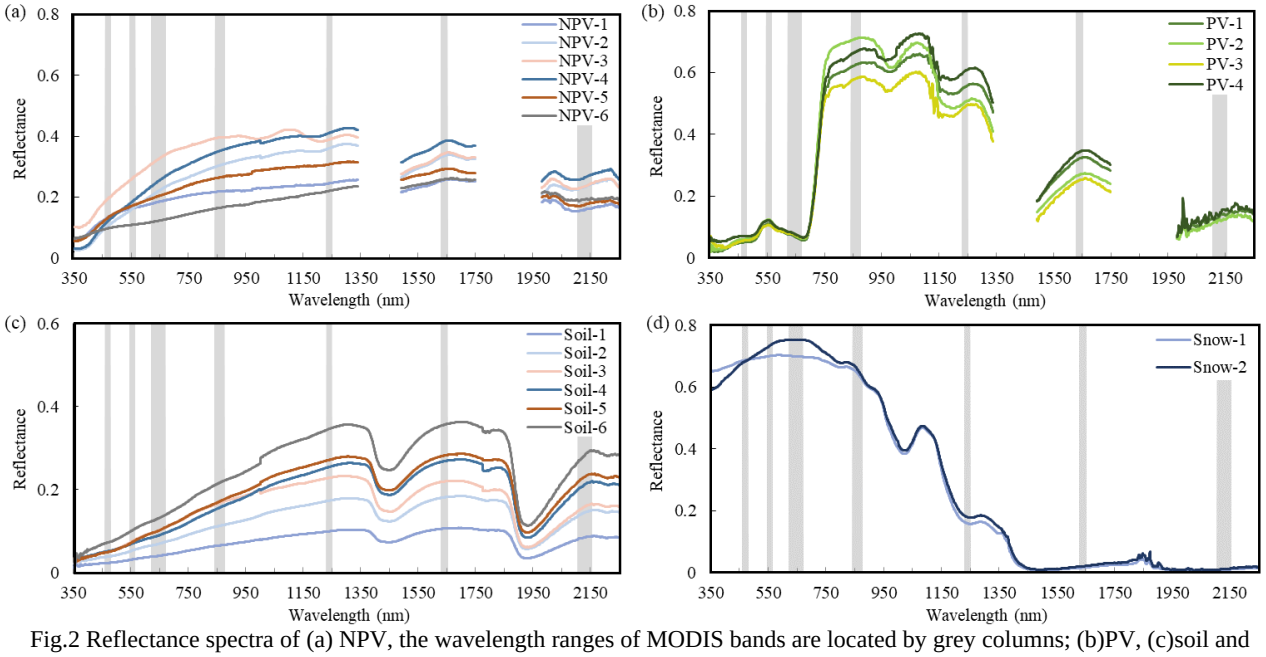

Fig.2 Reflectance spectra of (a) NPV, the wavelength ranges of MODIS bands are located by grey columns; (b)PV, (c)soil and (d)snow

Fig.4 shows the values of NPVI and DFI for different land cover components. It shows that NPVI can well distinguish NPV from PV, soil with different moisture, and snow. In contrast, DFI confuses NPV with the mixture of snow and wet soil.

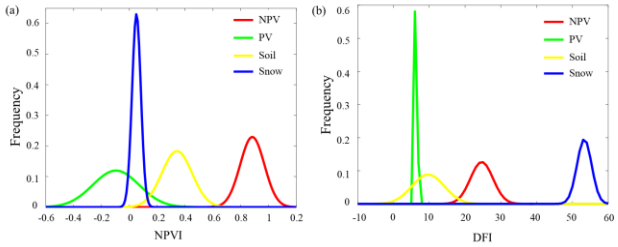

Fig.4 The distribution of NPVI (a) and DFI (b) for the four components

For the above simulated mixed data, NPVI shows a good linear correlation with NPV coverage (Fig. 5b). As a comparison, DFI shows much poorer correlation with simulated NPV coverage because of the influence of soil moisture and snow contamination (Fig. 5a).

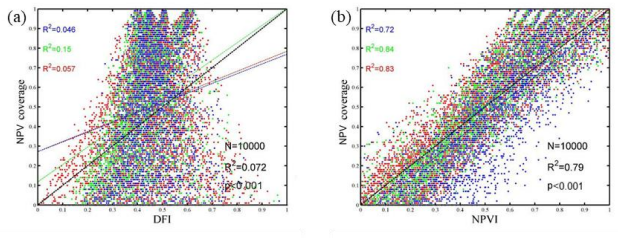

Fig.5 Relationship between NPV coverage and (a) DFI and (b) NPVI for the simulated data. Red, green and blue represent the different soil moisture ranging from 2.43% to 25.78%

3. RESULT

Field spectral experiments and plot investigated data were used for quantitatively validating the performance of NPVI at different scales. The validation results of DFI were also showed for comparation.

3.1 Validation result of field spectral experiment

To measure the sensitivity of NPVI to soil moisture, a group of NPV-soil mixed spectra were measured through a field experiment (Fig. 6). The NPV coverage varied from 0 to 1 and soil moisture set at 10%, 16% and 21%. Then, NPVI and DFI were calculated based on the measured mixed spectra through MODIS band simulation, respectively. As shown in Fig.7, NPVI (R^2 = 0.86) performs much better than DFI (R^2 = 0.086) in estimating NPV coverage. With the increase of soil moisture, the sensitivities of DFI and NPVI to NPV coverage become worse, whereas NPVI remains a good linear relationship with NPV coverage even in the wet soil background.

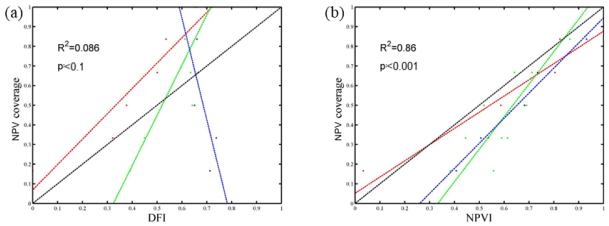

Fig.7 Relationship between NPV coverage and DFI (a), NPVI (b) in field experimental data. Red, green and blue respectively represent soil moisture of 11% ,16% and 21%.

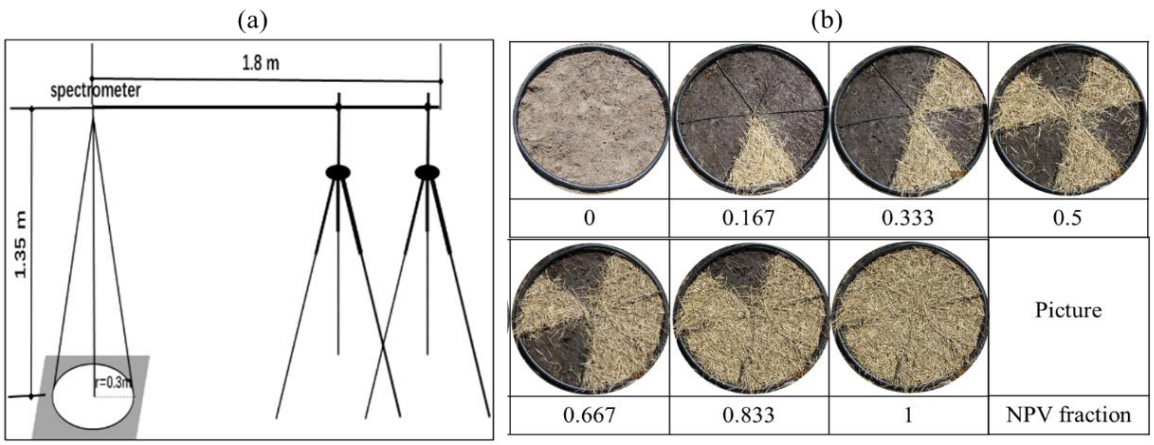

Fig. 6 (a) Experiment designment; (b) Samples with different NPV coverage

3.2 Validation result of field survey

In order to examine the performance of NPVI on a larger spatial scale, we checked the relationship of NPVI at MODIS pixels and the corresponding NPV coverage sampled through field survey. Field survey NPV coverage data at 64 plots were collected in the autumn of 2004, 2007 and 2017 (Fig. 8a) and the corresponding MOD09A1 reflectance at sample plots were extracted to calculate NPVI and DFI. The results show that NPVI is also better correlated with NPV than DFI in MODIS pixel scale (Fig. 9). The higher r-square of NPVI suggests its better relationship with NPV coverage even without snowmelt or wet soil background.

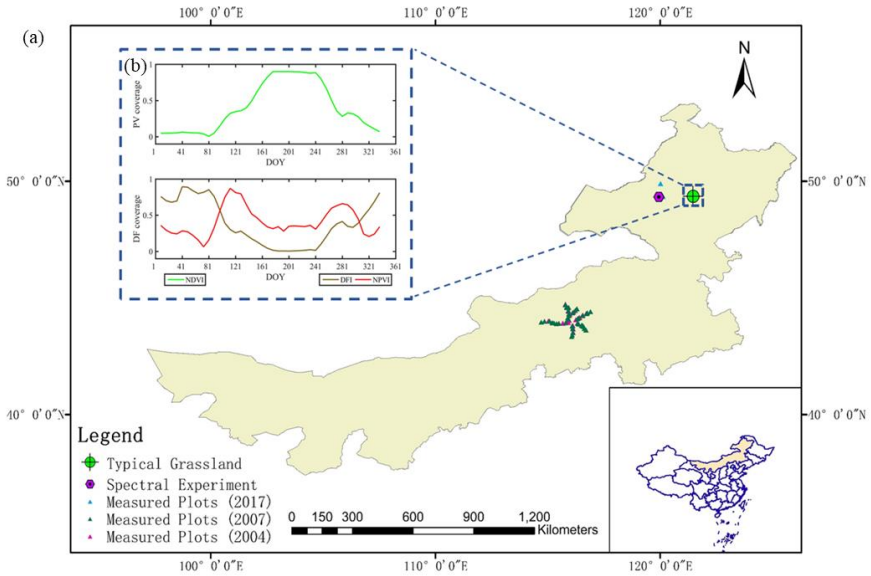

Fig.8 (a) Plots of field survey data, (b) Typical temporal profiles of NDVI, DFI and NPVI in typical grassland in 2017

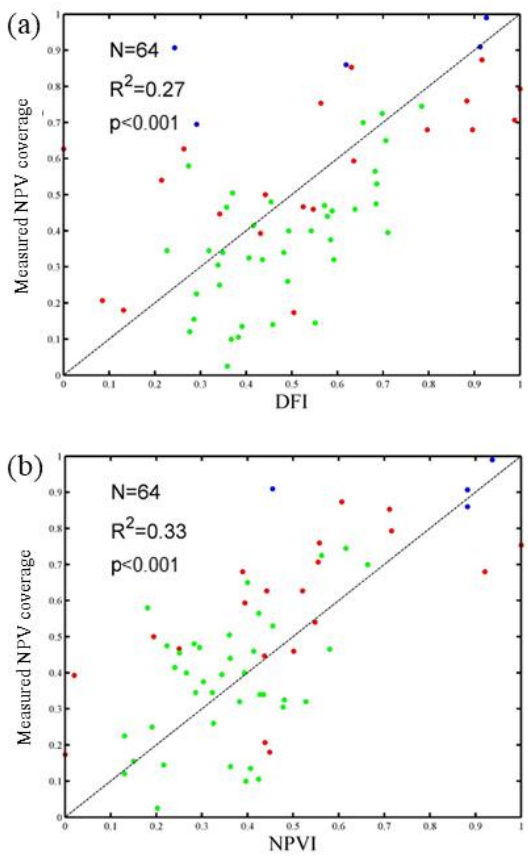

Fig.9 Relationship between measured NPV coverage and (a)DFI, (b)NPVI in 2004 (red), 2007(green) and 2017(blue)

3.3 Validation result of seasonal variation

Furthermore, the seasonal profiles of NPVI and DFI derived from MODIS data in 2017 shows that NPVI can capture the reasonable seasonal variation of NPV coverage (Fig.8b). As a reference, the NDVI time series (green line in Fig.8b) shows the variation of PV. In the growing season, both of DFI and NPVI are negatively correlated with NDVI because the vegetation growth could reduce the NPV coverage. NPVI is low in winter due to the snow contamination while DFI shows unreasonably high value because of its high value under snow cover background. The overestimation of NPV coverage could lead to misleading in the wildfire risk assessment in the winter. On the contrary, two peaks of NPVI in April and September correctly correspond to high-risk seasons of wildfire.

4. CONCLUSION AND DISCUSSION

The novel spectral linear transformation, developed from linear spectral mixed model of 4 components mixture of NPV, PV, soil and snow, can well estimate NPV coverage and capture the seasonal change of NPV coverage in north Asian steppe. This MODIS-based index, NPVI, was evaluated by field spectral experiment and field survey. Validation results suggests NPVI shows more robust performance than DFI. The time series of NPVI could help to monitor the wildfire risk and grazing intensity.

However, the NPVI still need further validations for applications. First, the selection of feature spectra in the linear spectral mixed model is mainly based on the north Asian steppe, and the performance of NPVI in other regions need more examinations. Second, it is lack of quantitative validation of the seasonal curve of NPVI. Thus, validations in more areas and more periods will be conducted in in the future.

ACKNOWLEDGEMENTS

This research was supported by National Natural Science Foundation of China under Grant 41871224.

REFERENCES

Elmore, A. J., Asner, G. P., & Hughes, R. F., 2005. Satellite monitoring of vegetation phenology and fire fuel conditions in Hawaiian drylands. Earth Interactions, 9(21), pp. 1-21. https://doi.org/10.1175/ei160.1

Daughtry C. S. T., Hunt E R, Doraiswamy P C, et al., 2005. Remote sensing the spatial distribution of crop residues[J]. Agronomy Journal, 97(3), pp. 864-871. https://doi.org/10.2134/agronj2003.0291

Nagler P L, Inoue Y, Glenn E P, et al., 2003. Cellulose absorption index (CAI) to quantify mixed soil–plant litter scenes[J]. Remote Sensing of Environment, 87(2-3), pp. 310-325. https://doi.org/10.1016/j.rse.2003.06.001

McNairn H, Protz R.,1993. Mapping corn residue cover on agricultural fields in Oxford County, Ontario, using Thematic Mapper[J]. Canadian Journal of Remote Sensing, 19(2), pp. 152-159. https://doi.org/10.1080/07038992.1993.10874543

Biard, F. and Baret, F., 1997, Crop residue estimation using multiband reflectance. Remote Sensing of Environment, 59, pp. 530–536. https://doi.org/10.1016/s0034-4257(96)00125-3

Van Deventer, A. P., et al., 1997, Using thematic mapper data to identify contrasting soil plains and tillage practices. Photogrammetric Engineering and Remote Sensing, 63, pp. 87-93.

Cao X, Chen J, Matsushita B, et al., 2010. Developing a MODIS-based index to discriminate dead fuel from photosynthetic vegetation and soil background in the Asian steppe area[J]. International Journal of Remote Sensing, 31(6), pp. 1589-1604. https://doi.org/10.1080/01431160903475274

Xu D, Guo X, Li Z, et al., 2014. Measuring the dead component of mixed grassland with Landsat imagery[J]. Remote Sensing of Environment, 142, pp. 33-43. https://doi.org/10.1016/j.rse.2013.11.017

Quemada M, Daughtry C S T., 2016. Spectral indices to improve crop residue cover estimation under varying moisture conditions[J]. Remote Sensing, 8(8), pp. 660. https://doi.org/10.3390/rs8080660